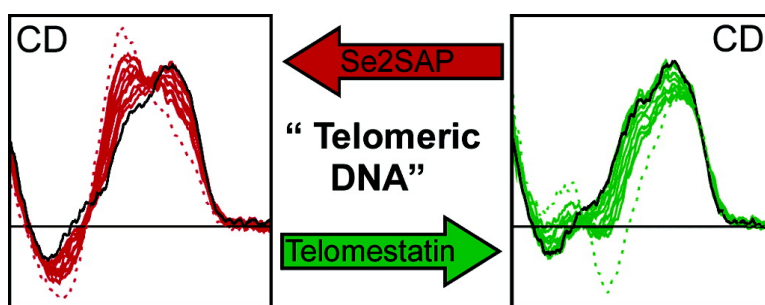


## Telomestatin and Diseleno Sapphyrin Bind Selectively to Two Different Forms of the Human Telomeric G-Quadruplex Structure

Evonne M. Rezler, Jeyaprakashnarayanan Seenisamy, Sridevi Bashyam, Mu-Yong Kim, Elizabeth White, W. David Wilson, and Laurence H. Hurley

*J. Am. Chem. Soc.*, **2005**, 127 (26), 9439-9447 • DOI: 10.1021/ja0505088 • Publication Date (Web): 09 June 2005

Downloaded from <http://pubs.acs.org> on March 25, 2009



### More About This Article

Additional resources and features associated with this article are available within the HTML version:

- Supporting Information
- Links to the 26 articles that cite this article, as of the time of this article download
- Access to high resolution figures
- Links to articles and content related to this article
- Copyright permission to reproduce figures and/or text from this article

[View the Full Text HTML](#)

## Telomestatin and Diselena Sapphyrin Bind Selectively to Two Different Forms of the Human Telomeric G-Quadruplex Structure

Evonne M. Rezler,<sup>†</sup> Jeyaprakashnarayanan Seenisamy,<sup>†</sup> Sridevi Bashyam,<sup>†</sup> Mu-Yong Kim,<sup>†</sup> Elizabeth White,<sup>‡</sup> W. David Wilson,<sup>‡</sup> and Laurence H. Hurley<sup>\*,†,§,||</sup>

Contribution from the College of Pharmacy, The University of Arizona, 1703 East Mabel, Tucson, Arizona 85721, Department of Chemistry, Georgia State University, Atlanta, Georgia 30303, Arizona Cancer Center, 1515 North Campbell Avenue, Tucson, Arizona 85724, Department of Chemistry, The University of Arizona, Tucson, Arizona 85721

Received January 25, 2005; E-mail: hurley@pharmacy.arizona.edu

**Abstract:** The human telomeric sequence d[T<sub>2</sub>AG<sub>3</sub>]<sub>4</sub> has been demonstrated to form different types of G-quadruplex structures, depending upon the incubation conditions. For example, in sodium (Na<sup>+</sup>), a basket-type G-quadruplex structure is formed. In this investigation, using circular dichroism (CD), biosensor-surface plasmon resonance (SPR), and a polymerase stop assay, we have examined how the addition of different G-quadruplex-binding ligands affects the conformation of the telomeric G-quadruplex found in solution. The results show that while telomestatin binds preferentially to the basket-type G-quadruplex structure with a 2:1 stoichiometry, 5,10,15,20-[tetra-(*N*-methyl-3-pyridyl)]-26-28-diselena sapphyrin chloride (Se2SAP) binds to a different form with a 1:1 stoichiometry in potassium (K<sup>+</sup>). CD studies suggest that Se2SAP binds to a hybrid G-quadruplex that has strong parallel and antiparallel characteristics, suggestive of a structure containing both propeller and lateral, or edgewise, loops. Telomestatin is unique in that it can induce the formation of the basket-type G-quadruplex from a random coil human telomeric oligonucleotide, even in the absence of added monovalent cations such as K<sup>+</sup> or Na<sup>+</sup>. In contrast, in the presence of K<sup>+</sup>, Se2SAP was found to convert the preformed basket G-quadruplex to the hybrid structure. The significance of these results is that the presence of different ligands can determine the type of telomeric G-quadruplex structures formed in solution. Thus, the biochemical and biological consequences of binding of ligands to G-quadruplex structures found in telomeres and promoter regions of certain important oncogenes go beyond mere stabilization of these structures.

### Introduction

Telomeres are specialized, functional DNA–protein structures found at the ends of all eukaryotic linear chromosomes.<sup>1</sup> They help to protect the ends of chromosomes from being treated like damaged DNA needing repair, and they also provide a means of complete replication of the chromosome.<sup>2</sup> Mammalian telomeres comprise a long stretch of simple tandem repeats of the G-tract sequence (TTAGGG/CCCTAA)<sub>n</sub> and a short, single-stranded G-rich 3′-overhang.<sup>1c,d</sup> Telomeres consist of tandem arrays of telomeric TTAGGG repeats complexed with specific

DNA binding proteins.<sup>1f</sup> Among them, TRF1 and TRF2 are known to bind to the double-stranded telomeric TTAGGG repeats,<sup>1g</sup> while the single-stranded telomeric DNA at the 3′-end is specifically bound by hPot1.<sup>1h</sup> Dividing cells have been shown to undergo a progressive loss of 50–200 bases following every cell division due to incomplete replication of the lagging strand. This process eventually leads to critically short telomeres and ultimately triggers cell cycle arrest or cell death.<sup>3</sup> Under rare circumstances, a cell can become immortal when the enzyme telomerase becomes active and serves to indefinitely stabilize the length of its telomeres by the addition of telomeric DNA repeats onto the 3′-ends of the single-stranded telomeres.<sup>4</sup> Importantly, telomerase is active in a majority of human cancer cells but is inactive in most normal somatic cells,<sup>5</sup> and therefore the inhibition of telomerase has become an attractive strategy for the design of anticancer drugs. The use of drugs to target

<sup>†</sup> College of Pharmacy, The University of Arizona.

<sup>‡</sup> Georgia State University.

<sup>§</sup> Arizona Cancer Center.

<sup>||</sup> Department of Chemistry, The University of Arizona.

- (1) (a) Allshire, R. C.; Dempster, M.; Hastie, N. D. *Nucleic Acids Res.* **1989**, *17*, 4611. (b) de Lange, T.; Shiue, L.; Myers, R. M.; Cox, D. R.; Naylor, S. L.; Killery, A. M.; Varmus, H. E. *Mol. Cell. Biol.* **1990**, *10*, 518. (c) Makarov, V. L.; Hirose, Y.; Langmore, J. P. *Cell* **1997**, *88*, 657. (d) McElligott, R.; Wellinger, R. J. *EMBO J.* **1997**, *16*, 3705. (e) Griffith, J. D.; Comeau, L.; Rosenfield, S.; Stansel, R. M.; Bianchi, A.; Moss, H.; de Lange, T. *Cell* **1999**, *97*, 503. (f) Mattern, K. A.; Swiggers, S. J.; Nigg, A. L.; Lowenberg, B.; Houtsmuller, A. B.; Zijlmans, J. M. *Mol. Cell Biol.* **2004**, *24*, 5587. (g) Karlseder, J. *Cancer Lett.* **2003**, *194*, 189. (h) Lei, M.; Podell, E. R.; Cech, T. R. *Nat. Struct. Mol. Biol.* **2004**, *11*, 1223.
- (2) (a) van Steensel, B.; Smogorzewska, A.; de Lange, T. *Cell* **1998**, *92*, 401. (b) Blackburn, E. H. *Nature* **2000**, *408*, 53.

(3) (a) Harley, C. B.; Futcher, A. B.; Greider, C. W. *Nature* **1990**, *345*, 458.

(b) Smogorzewska, A.; de Lange, T. *EMBO J.* **2002**, *21*, 4338.

(4) Healy, K. C. *Oncol. Res.* **1995**, *7*, 121.

(5) (a) Shay, J. W.; Bacchetti, S. *Eur. J. Cancer* **1997**, *33*, 787. (b) Mergny, J.-L.; Riou, J.-F.; Mailliet, P.; Teulade-Fichou, M.-P.; Gilson, E. *Nucleic Acids Res.* **2002**, *30*, 839.

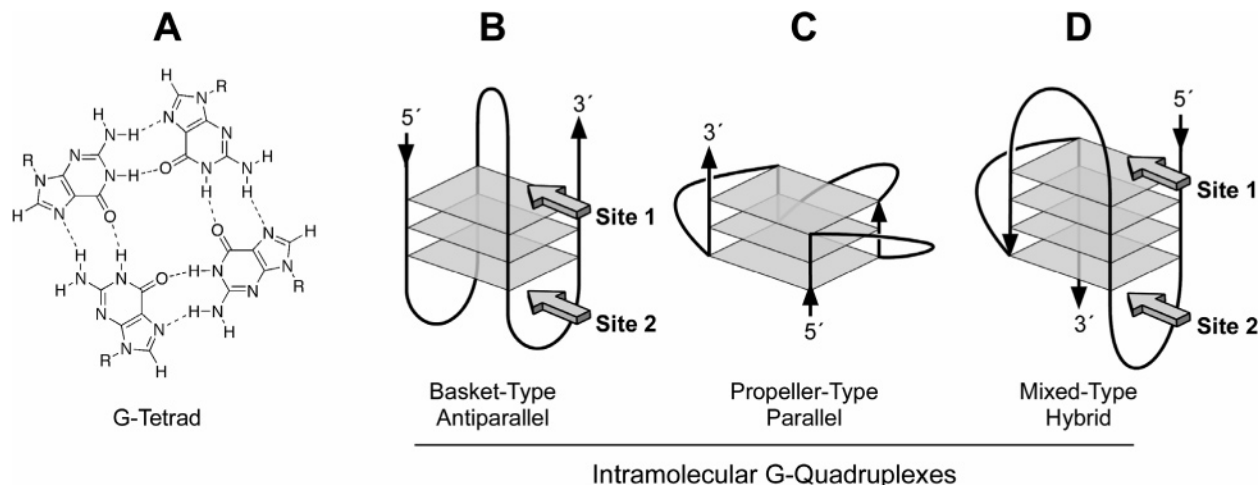


**Figure 1.** Structures of the G-tetrad and the three types of intramolecular G-quadruplex structures previously found for telomeric DNA sequences.

the substrate of telomerase is emerging as a promising approach to the inhibition of telomerase activity.<sup>5b,6</sup>

The single-stranded G-tract human telomeric DNA can fold to form a secondary DNA structure that has three stacked guanine tetrads (Figure 1A), and this structure is termed an intramolecular G-quadruplex. To date, two intramolecular G-quadruplex structures have been characterized for the human telomeric sequence as either basket-type or propeller-type, depending on the incubation conditions (Figure 1, parts B and C, respectively). Wang and Patel reported that a DNA oligonucleotide with a human telomeric sequence forms an intramolecular basket-type G-quadruplex structure in the presence of Na<sup>+</sup>.<sup>7</sup> Basket-type G-quadruplexes have one diagonal and two lateral, or edgewise, loop regions, with the guanine columns in an antiparallel arrangement.<sup>8</sup> More recently, Parkinson et al. reported a solid-state, intramolecular propeller-type G-quadruplex structure that forms in the presence of K<sup>+</sup>.<sup>9</sup> Propeller-type G-quadruplexes have no loop regions available for end-stacking of G-quadruplex ligands, and their guanine columns are also in a homogeneous parallel arrangement.<sup>8</sup> The distinctive three-dimensional appearance of these loops in a propeller-like configuration has led to their novel name.

In addition to the basket- and propeller-type G-quadruplex conformations that can form from human telomeric DNA in solution and solid forms, respectively, another study has suggested alternative mixtures, including only antiparallel conformations in K<sup>+</sup>- and Na<sup>+</sup>-containing solutions in the presence of platinum cross-linking.<sup>10</sup> In a more recent study, two antiparallel and one parallel conformation were proposed to coexist in solution.<sup>11</sup> In the latter study, <sup>125</sup>I-radioprobeing was used in conjunction with DNA strand breaks to predict the conformations present under different salt concentrations. This same study has the advantage that no external ligand was

involved in the incubation, and it was carried out in solution conditions so that the equilibrium would not be affected by ligands or crystal packing forces.

One other intramolecular secondary structure study of a telomeric sequence has been previously reported in the literature, and it is a solution NMR structure determination of the *Tetrahymena* telomeric DNA sequence, which is very similar to that of the human telomeric DNA but contains a TTGGGG repeating motif instead of the human telomeric TTAGGG motif.<sup>12</sup> In this study, Wang and Patel found that the *Tetrahymena* oligonucleotide forms a mixed-type hybrid structure containing two lateral loops and one propeller loop (Figure 1D).

The formation of human telomeric G-quadruplexes has been shown to inhibit telomerase activity due to the sequestration of the single-stranded d[T<sub>2</sub>AG<sub>3</sub>]<sub>n</sub> primer molecules.<sup>13</sup> Indeed, a number of small molecules have been previously found that stabilize human telomeric G-quadruplex structures and therefore inhibit telomerase activity, most probably via this primer sequestration mechanism.<sup>6a</sup> Some of these compounds have also exhibited encouraging biological effects in vitro that go beyond telomerase inhibition, including telomeric disruption, formation of anaphase bridges, apoptosis, and in vivo activity in mouse xenograft models.<sup>14</sup>

(12) Wang, Y.; Patel, D. J. *Structure* **1994**, *2*, 1141.

(13) Zahler, A. M.; Williamson, J. R.; Cech, T. R.; Prescott, D. M. *Nature* **1991**, *350*, 718.

(14) (a) Izbicka, E.; Nishioka, D.; Marcell, V.; Raymond, E.; Davidson, K. K.; Lawrence, R. A.; Wheelhouse, R. T.; Hurley, L. H.; Wu, R. S.; Von Hoff, D. D. *Anti-Cancer Drug Des.* **1999**, *14*, 355. (b) Izbicka, E.; Wheelhouse, R. T.; Raymond, E.; Davidson, K. K.; Lawrence, R. A.; Sun, D.; Windle, B. E.; Hurley, L. H.; Von Hoff, D. D. *Cancer Res.* **1999**, *59*, 639. (c) Gowan, S. M.; Heald, R.; Stevens, M. F. G.; Kelland, L. R. *Mol. Pharmacol.* **2001**, *60*, 981. (d) Duan et al. *Mol. Cancer Ther.* **2001**, *1*, 103. (e) Grand, C. L.; Han, H.; Muñoz, R. M.; Weitman, S.; Von Hoff, D. D.; Hurley, L. H.; Bearss, D. J. *Mol. Cancer Ther.* **2002**, *1*, 565. (f) Kim, M.-Y.; Duan, W.; Gleason-Guzman, M.; Hurley, L. H. *J. Med. Chem.* **2003**, *46*, 571. (g) Read, M.; Harrison, R. J.; Romagnoli, B.; Tanius, F. A.; Gowan, S. H.; Reszka, A. P.; Wilson, W. D.; Kelland, L. R.; Neidle, S. *Proc. Natl. Acad. Sci. U.S.A.* **2001**, *98*, 4844. (h) Riou, J. F.; Guittat, L.; Mailliet, P.; Laoui, A.; Renou, E.; Petitgenet, O.; Megnin-Chanet, F.; Hélène, C.; Mergny, J. L. *Proc. Natl. Acad. Sci. U.S.A.* **2002**, *99*, 2672. (i) Heald, R. A.; Modi, C.; Cookson, J. C.; Hutchinson, I.; Loughton, C. A.; Gowan, S. M.; Kelland, L. R.; Stevens, M. F. G. *J. Med. Chem.* **2002**, *45*, 590. (j) Gowan, S. M.; Harrison, J. R.; Patterson, L.; Valenti, M.; Read, M. A.; Neidle, S.; Kelland, L. R. *Mol. Pharmacol.* **2002**, *61*, 1154. (k) Shammas, M. A.; Shmookler Reis, R. J.; Akiyama, M.; Koley, H.; Chauhan, D.; Hideshima, T.; Goyal, R. K.; Hurley, L. H.; Anderson, K. C.; Munshi, N. C. *Mol. Cancer Ther.* **2003**, *2*, 825. (l) Shammas, M. A.; Shmookler Reis, R. J.; Li, C.; Koley, H.; Hurley, L. H.; Anderson, K. C.; Munshi, N. C. *Clin. Cancer Res.* **2004**, *10*, 770.

(6) (a) Sun, D.; Thompson, B.; Cathers, B. E.; Salazar, M.; Kerwin, S. M.; Trent, J. O.; Jenkins, T. C.; Neidle, S.; Hurley, L. H. *J. Med. Chem.* **1997**, *40*, 2113. (b) Kerwin, S. M. *Curr. Pharm. Des.* **2000**, *6*, 441. (c) Rezler, E. M.; Bearss, D. J.; Hurley, L. H. *Curr. Opin. Pharmacol.* **2002**, *2*, 415. (d) Neidle, S.; Parkinson, G. *Nat. Rev. Drug Discovery* **2002**, *1*, 383. (e) Rezler, E. M.; Bearss, D. J.; Hurley, L. H. *Annu. Rev. Pharmacol. Toxicol.* **2003**, *43*, 359.

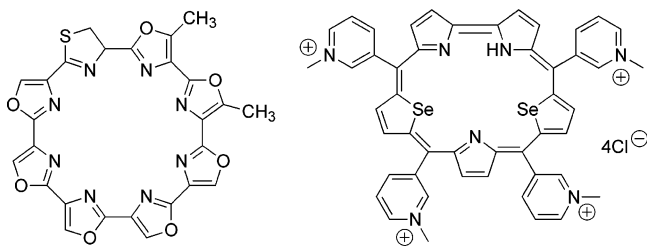
(7) Wang, Y.; Patel, D. J. *Structure* **1993**, *1*, 263.

(8) Patel, D. J. *Nature* **2002**, *417*, 807.

(9) Parkinson, G. N.; Lee, M. P.; Neidle, S. *Nature* **2002**, *417*, 876.

(10) Redon, S.; Bombard, S.; Elizondo-Riojas, M.-A.; Chottard, J.-C. *Nucleic Acids Res.* **2003**, *31*, 1605.

(11) He, Y.; Neumann, R. D.; Panyutin, I. G. *Nucleic Acids Res.* **2004**, *32*, 5359.



Telomestatin

Se2SAP

**Figure 2.** Structures of the G-quadruplex-binding drugs telomestatin and Se2SAP.

Telomestatin (Figure 2) is a natural product isolated from *Streptomyces anulatus* 3533-SV4, which has been shown to be a very potent telomerase inhibitor through its strong G-quadruplex interaction.<sup>15</sup> We have previously demonstrated that telomestatin interacts quite strongly and specifically with human telomeric intramolecular G-quadruplexes and also has a 70-fold selectivity for intramolecular G-quadruplex structures over duplex DNA.<sup>16</sup> Importantly, we also found that telomestatin was able to induce and stabilize G-quadruplexes in the absence of added monovalent cations, which is a unique characteristic among G-quadruplex-interactive compounds.<sup>16</sup> In addition, the results from our previous molecular modeling study showed that the minimized binding energy when two telomestatin molecules were bound per one G-quadruplex was lower than when one telomestatin molecule was bound, and the telomestatin molecules were proposed to bind by end-stacking in the loop regions of this G-quadruplex rather than by intercalation between the G-tetrads.<sup>15b</sup> The compound Se2SAP (Figure 2) is a synthetic, core-modified, expanded porphyrin that was first synthesized in our laboratory with the specific aim of targeting G-quadruplex DNA structures that could be formed by DNA *in vivo*, whether it be at the ends of telomeres or in the G-rich promoter regions of oncogenes.<sup>17</sup> It is likely that this molecule also has an end-stacking-type of binding propensity in the diagonal and lateral loop regions of G-quadruplexes, which can be attributed to the planar structure of this molecule.<sup>18</sup>

In the current study, we used CD spectroscopy to demonstrate that for the human telomeric d[T<sub>2</sub>AG<sub>3</sub>]<sub>4</sub> oligonucleotide, telomestatin can convert, under certain conditions, the preformed mixed-type hybrid G-quadruplex to the antiparallel basket form, while Se2SAP can convert the preformed basket-type G-quadruplex to a hybrid G-quadruplex structure. We also confirm that telomestatin can induce the formation of the basket-type intramolecular G-quadruplex formed from the d[T<sub>2</sub>AG<sub>3</sub>]<sub>4</sub> oligonucleotide in the absence of significant concentrations of added cations, and we determine the stoichiometry for this reaction. Furthermore, we provide further experimental evidence for the structure-based selectivity of these two compounds using a *Taq* polymerase stop assay and SPR under varied salt conditions.

## Experimental Procedures

**Materials, Enzymes, Oligonucleotides, and Drugs.** Acrylamide/bisacrylamide solution and ammonium persulfate were purchased from Bio-Rad, and *N,N,N',N'*-tetramethylethylenediamine was purchased from Fisher. T4 polynucleotide kinase and *Taq* DNA polymerase were purchased from New England Biolabs and Promega, respectively. [ $\gamma$ -<sup>32</sup>P]ATP was purchased from NEN Dupont. The desalted and deprotected DNA primer d[TAATACGACTCACTATAGCAAT-TGCGTG] and the human telomeric template sequence d[TCC-AACTATGTATAC(TTAGGG)<sub>4</sub>TTAGCGGCACGCAATTGCTAT-AGTGAGTCGTATTA] were obtained from Sigma Genosys and dissolved in double-distilled water to be used without further purification. Stock solutions of telomestatin and Se2SAP (10 mM) were made using DMSO (10%) and double-distilled water, respectively. Further dilutions to working concentrations were made with double-distilled water immediately prior to use.

**CD Spectroscopy.** CD spectra were recorded on a Jasco-810 spectropolarimeter (Jasco, Easton, MD) using a quartz cell of 1-mm optical path length and an instrument scanning speed of 100 nm/min with a response time of 1 s, and over a wavelength range of 200–330 nm. All DNA samples were dissolved in Tris buffer (50 mM, pH 7.6). Telomestatin and Se2SAP were dissolved from the 10 mM stock solutions to a concentration of 0.5 mM with water and titrated into the DNA samples at 0.5 mol equiv up to 5 mol equiv (the 10 mM stock solution of telomestatin was made up in 10% DMSO, while water was used for Se2SAP). Where appropriate, the samples also contained 100 mM KCl and/or NaCl. The DNA strand concentrations used were 12.5  $\mu$ M, and the CD data are a representation of four averaged scans taken at 25 °C. All CD spectra are baseline-corrected for signal contributions due to the buffer and for buffer and DMSO for the samples containing telomestatin.

***Taq* Polymerase Stop Assay.** The DNA primer d[TAATACGACTCACTATAGCAATTGCGTG] was 5'-end-labeled by incubating with T4 polynucleotide kinase and [ $\gamma$ -<sup>32</sup>P]ATP at 37 °C for 1 h. The end-labeled DNA was then purified on a Bio-Spin 6 chromatography column (Bio-Rad) after inactivation of the T4 kinase by heating at 70 °C for 8 min. The labeled primer (100 nM) and template DNA (100 nM) were then annealed in an annealing buffer [50 mM Tris-HCl (pH 7.5), 10 mM NaCl] by heating to 95 °C and then slowly cooling to room temperature. DNA formed by annealing the primer to the template sequence was purified using gel electrophoresis on a 12% native polyacrylamide gel. The purified DNA was then diluted to a concentration of 2 nM and mixed with the reaction buffer (10 mM MgCl<sub>2</sub>, 0.5 mM DTT, 0.1 mM EDTA, 1.5  $\mu$ g/ $\mu$ L BSA) and 0.1 mM dNTP. Where appropriate, KCl and/or NaCl solutions (to a final concentration of 100 mM per sample) were also added. The reaction mixtures were incubated for 20 min at room temperature with various concentrations of drugs, and then *Taq* DNA polymerase was added to each sample, which were further incubated at an elevated polymerase extension temperature of 35 °C for 30 min. The polymerase extension was stopped by adding 2 $\times$  stop buffer (10 mM EDTA, 10 mM NaOH, 0.1% xylene cyanole, 0.1% bromophenol blue in formamide solution), and the samples were analyzed on a 16% denaturing gel.

**Immobilization of DNA and SPR Experiments.** The 5'-biotin-AGGG(TTAGGG)<sub>3</sub>-3' telomere DNA sequence (Midland Certified Reagent Co.) used in the SPR experiments was HPLC purified. The SPR binding experiments were performed with a four-channel BIAcore 3000 optical biosensor system (BIAcore, Inc.). To conduct the binding experiments, the biotin-labeled DNA was bound to a streptavidin-coated sensorchip (BIAcore SA with streptavidin covalently linked to the chip through carboxymethyl dextran) as previously described.<sup>17</sup> One flow cell was used to immobilize the DNA, while a second cell was left blank as a control. The binding experiments were performed in two different sterile filtered and degassed HBS buffers: 0.01 M HEPES (pH 7.4), 3 mM EDTA, and 0.005% surfactant P20 with either 0.1 M KCl or 0.1 M NaCl. For binding experiments, a stock solution of Se2SAP was

- (15) (a) Shin-ya, K.; Wierzbza, K.; Matsuo, K.; Ohtani, T.; Yamada, Y.; Furihata, K.; Hayakawa, Y.; Seto, H. *J. Am. Chem. Soc.* **2001**, *123*, 1262. (b) Kim, M.-Y.; Vankayalapati, H.; Shin-ya, K.; Wierzbza, K.; Hurley, L. H. *J. Am. Chem. Soc.* **2002**, *124*, 2098.  
 (16) Kim, M.-Y.; Gleason-Guzman, M.; Izbicka, E.; Nishioka, D.; Hurley, L. H. *Cancer Res.* **2003**, *63*, 3247.  
 (17) Seenisamy, J.; Bashyam, S.; Gokhale, V.; Vankayalapati, H.; Grand, C. L.; Siddiqui-Jain, A.; Streiner, N.; Wilson, W. D.; Hurley, L. H. *J. Am. Chem. Soc.* **2005**, *127*, 2944–2959.  
 (18) Haider, S. M.; Parkinson, G. N.; Neidle, S. *J. Mol. Biol.* **2003**, *326*, 117.



prepared at a 1 mM concentration in water, and experimental concentrations were prepared in the desired buffer by serial dilutions from stock solution. The experimental solutions at concentrations from 1 to 1000 nM were injected through the DNA and blank flow cells at a rate of 50  $\mu\text{L}/\text{min}$  at 25  $^{\circ}\text{C}$  until a constant steady-state response was obtained. Compound solution flow was then replaced by buffer flow, resulting in dissociation of the complex. To remove any remaining bound compound after the dissociation phase of the sensorgram, a low pH glycine regeneration buffer was used (10 mM glycine at pH 2). The baseline was then reestablished, and the next compound concentration sample was injected.

The reference response from the blank cell was subtracted from the response of the sample flow cell to give an instrument response (RU = resonance units) that is directly proportional to the amount of Se2SAP bound to the immobilized DNA. The steady-state response at each concentration was determined by linear averaging over a 10–20 s or longer time span, depending on the length of the steady-state plateau. This steady-state response was then plotted against the concentration of the free compound (determined by the compound concentration in the flow solution) in equilibrium with the complex ( $C_{\text{free}}$ ). The number of binding sites as well as the binding affinity were calculated by fitting the data to the following two-site interaction model using Kaleidagraph for nonlinear least squares optimization of the binding parameters, where  $\text{RU}_{\text{max}}$  was the maximum response per bound compound and  $K_1$  and  $K_2$  were the macroscopic binding constants for a two-site binding model:

$$\text{RU} = \text{RU}_{\text{max}} * (K_1 * C_{\text{free}} + 2 * K_1 * K_2 * C_{\text{free}}^2) / (1 + K_1 * C_{\text{free}} + K_1 * K_2 * C_{\text{free}}^2)$$

A single-site binding model was obtained by setting  $K_2$  in the equation above to zero. The  $\text{RU}_{\text{max}}$  value could also be calculated from the amount of DNA bound to the surface<sup>19</sup> and served as an internal control for the fitting results. Errors in fitting two  $K$  values within any experiment were  $\pm 10\%$ , while errors in  $K$  values in replicate experiments were  $\pm 25\%$ . Errors in fitting results that required only a single  $K$  value were  $\pm 10\%$ .

## Results

### 1. Circular Dichroism Studies. 1.1. Telomestatin. 1.1.1. Telomestatin Selectively Induces the Formation of the Antiparallel Basket-Type Intramolecular G-Quadruplex from the Human Telomeric Oligonucleotide in the Absence of Added Salt.

The telomestatin-induced formation of the human telomeric intramolecular G-quadruplex structure in the absence of added  $\text{K}^+$  or  $\text{Na}^+$  was monitored using CD spectroscopy (Figure 3). In the absence of telomestatin, the CD spectrum of the human telomeric  $\text{d}[\text{T}_2\text{AG}_3]_4$  oligonucleotide was found to have a negative band centered at 238 nm, a major positive band at 257 nm, and a minor negative band at 280 nm (Figure 3, solid black line). However, upon addition of excess telomestatin (5 mol equiv) to the  $\text{d}[\text{T}_2\text{AG}_3]_4$  oligonucleotide, a dramatic change in the CD spectrum was observed. The bands at 238, 257, and 280 nm disappeared, while a major positive band centered at 292 nm, a negative band at 262 nm, and a minor positive band at 245 nm appeared (Figure 3, dashed black line). Approximately 15 min after the addition of telomestatin, the new peaks and troughs ceased to increase in elliptic intensity, and the reaction probably reached, or was very close to, the equilibrium state. These dramatic changes in the CD spectrum of the human telomeric  $\text{d}[\text{T}_2\text{AG}_3]_4$  oligonucleotide after the addition of telomestatin are consistent with this drug binding

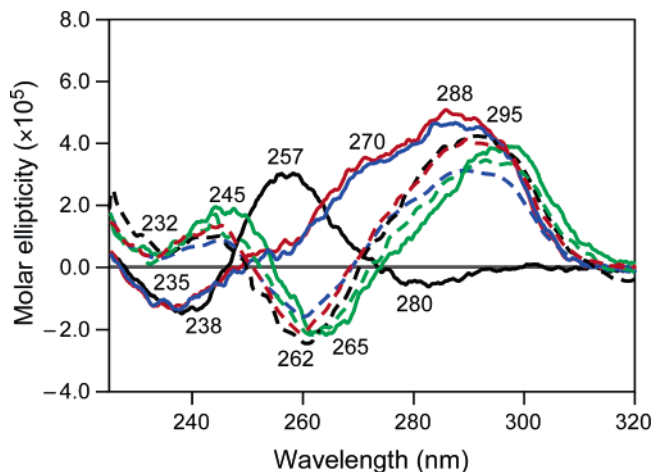


**Figure 3.** CD spectra of  $\text{d}[\text{T}_2\text{AG}_3]_4$  with  $\text{Na}^+$  and/or  $\text{K}^+$  and telomestatin. Incubation times are as described in the Experimental Procedures. Line colors: solid black =  $\text{d}[\text{T}_2\text{AG}_3]_4$  (no salt added); dashed black =  $\text{d}[\text{T}_2\text{AG}_3]_4$  + telomestatin (no salt added); solid red =  $\text{d}[\text{T}_2\text{AG}_3]_4$  + 100 mM KCl; dashed red =  $\text{d}[\text{T}_2\text{AG}_3]_4$  + 100 mM KCl + telomestatin; solid green =  $\text{d}[\text{T}_2\text{AG}_3]_4$  + 100 mM NaCl; dashed green =  $\text{d}[\text{T}_2\text{AG}_3]_4$  + 100 mM NaCl + telomestatin; solid blue =  $\text{d}[\text{T}_2\text{AG}_3]_4$  + 100 mM KCl + 100 mM NaCl; dashed blue =  $\text{d}[\text{T}_2\text{AG}_3]_4$  + 100 mM KCl + 100 mM NaCl + telomestatin.

to the DNA and thus causing substantial change(s) in the conformation of the DNA. In fact, the CD spectrum of this new DNA conformation is virtually identical to the CD spectra of antiparallel G-quadruplexes described in previous studies, where the major positive band was usually observed around 290 nm with a negative band at 265 nm and a smaller positive band at 246 nm.<sup>20</sup> Importantly, in these previous studies the G-quadruplexes were characterized as intramolecular basket-type structures using CD as well as NMR, EMSA, and DMS footprinting and other chemical probing studies.<sup>7,20,21</sup> As anticipated, upon addition of 100 mM NaCl to the  $\text{d}[\text{T}_2\text{AG}_3]_4$  telomeric oligomer in the absence of telomestatin, the CD spectrum exhibits a maxima–minima pattern similar, but not identical, to that described with addition of telomestatin: a major positive band around 290 nm, a negative band at 265 nm, and a minor positive band at 245 nm (Figure 3, solid green line).

### 1.1.2. The Stoichiometry of Binding of Telomestatin to the Human Telomeric Basket-Type G-Quadruplex is 2:1.

A CD titration was carried out in the absence of salt to determine the stoichiometry for telomestatin binding to the human telomeric G-quadruplex structure. A sample of the  $\text{d}[\text{T}_2\text{AG}_3]_4$  at a strand concentration of 25  $\mu\text{M}$  was titrated with 0.5 mol equiv of telomestatin (1 mM solution). After each addition of telomestatin, the reaction was allowed to equilibrate for at least 15 min (until no elliptic changes were observed) and a CD spectrum was collected. The resulting nine spectra were plotted and are shown in Figure 4A (where the arrow directions indicate the progressive evolution or disappearance of CD signal). The band at 257 nm decreased in ellipticity with each addition of telomestatin, while the band at 292 nm appeared and appreciably increased in ellipticity until a ratio of 2:1 for telomestatin to  $\text{d}[\text{T}_2\text{AG}_3]_4$  was reached. The changes in ellipticity at these two

(19) Davis, T. M.; Wilson, W. D. *Anal. Biochem.* **2000**, *284*, 348.

(20) (a) Balagurumoorthy, P.; Brahmachari, S. K. *J. Biol. Chem.* **1994**, *269*, 21858. (b) Giraldo, R.; Suzuki, M.; Chapman, L.; Rhodes, D. *Proc. Natl. Acad. Sci. U.S.A.* **1994**, *91*, 7658. (c) Mergny, J. L.; Maurizot, J. C. *ChemBioChem* **2001**, *2*, 124. (d) Li, W.; Wu, P.; Ohmichi, T.; Sugimoto, N. *FEBS Lett.* **2002**, *526*, 77.

(21) Smith, F. W.; Feigon, J. *Nature* **1992**, *356*, 164.

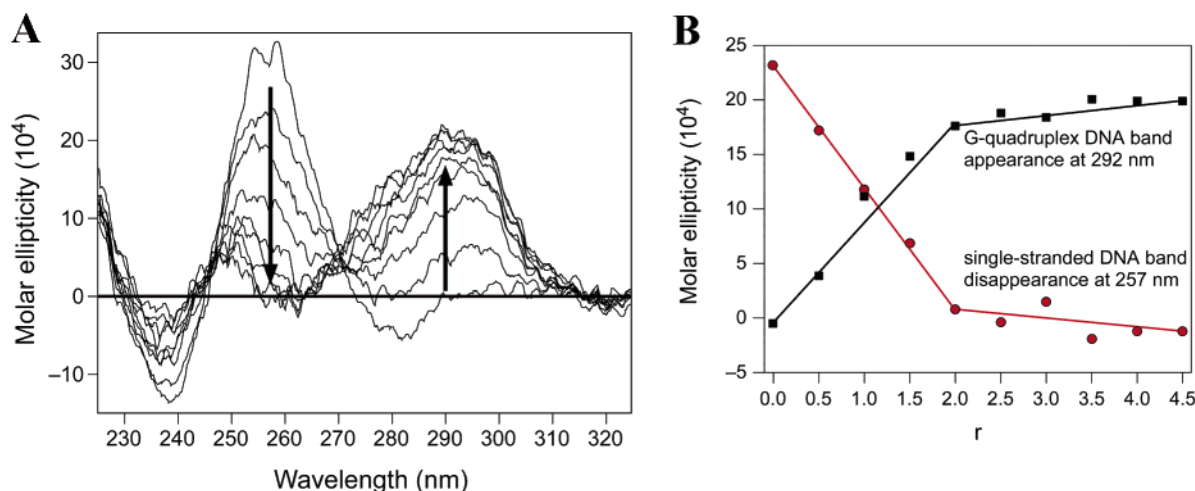


**Figure 4.** (A) A stacked plot representing the CD titration of the d[T<sub>2</sub>AG<sub>3</sub>]<sub>4</sub> with half equivalents of telomestatin (spectra collected at 25 °C). (B) Two titration curves representing the changes in ellipticity with the addition of each telomestatin half equivalent as monitored at 257 and 292 nm. An inflection point is observed for the two curves at  $r = 2$  (where  $r$  is the telomestatin/DNA fraction).

wavelengths (257 and 292 nm, where the greatest changes in ellipticity were observed in nonmaxima regions) as a function of telomestatin/DNA fraction ( $r$ ) are plotted in Figure 4B. An inflection point observed in each graph when  $r = 2$  is consistent with the formation of a 2:1 telomestatin–oligonucleotide complex, and the CD spectrum of this complex is also consistent with an antiparallel G-quadruplex structure of the basket-type being adopted by the DNA (as discussed in the previous section).

**1.1.3. Telomestatin Selectively Converts the Preformed Mixed-Type Hybrid G-Quadruplex to the Antiparallel Basket-Type G-Quadruplex in the Presence of K<sup>+</sup>.** The conformational characteristics of the human telomeric d[T<sub>2</sub>AG<sub>3</sub>]<sub>4</sub> oligonucleotide were compared under different salt conditions using CD spectroscopy (Figure 3). Upon addition of 100 mM of Na<sup>+</sup> or K<sup>+</sup> to a 12.5 μM solution of d[T<sub>2</sub>AG<sub>3</sub>]<sub>4</sub> in Tris buffer (pH 7.6), quite distinct transformations of the CD spectra were observed, with strong positive peaks appearing centered at 295 and 288 nm for the Na<sup>+</sup> and K<sup>+</sup> conditions, respectively (Figure 3 solid green and red lines, respectively). The CD spectrum of the oligonucleotide with Na<sup>+</sup> also contained a moderately strong negative band at 265 nm and a smaller positive band at 245 nm, and as described before, this spectrum closely resembles that of the human telomeric oligonucleotide with telomestatin in the absence of salt. In contrast, the CD spectrum of the oligonucleotide with K<sup>+</sup> had a distinctive shoulder located near 270 nm on the strong positive band at 288 nm, and a small negative peak was also present near 235 nm. This spectrum is considerably different, particularly in the region below 280 nm, from the spectra obtained under Na<sup>+</sup> conditions, even when telomestatin was present (dashed green line). The presence of the strong maximum at 288 and the shoulder at 270 nm, as well as the spectral characteristic of a parallel G-quadruplex below 280 nm, suggests that the structure formed in K<sup>+</sup> is a G-quadruplex that contains mixed parallel/antiparallel components or that there is a mixture of G-quadruplex structures that have parallel and antiparallel characteristics.

When both Na<sup>+</sup> and K<sup>+</sup> were added simultaneously to the human telomeric oligonucleotide, the resulting CD spectrum observed (Figure 3, solid blue line) was virtually identical to the CD spectrum of the oligonucleotide under K<sup>+</sup> conditions without telomestatin (Figure 3, solid red line). Upon the addition

of excess telomestatin to the oligonucleotide containing either K<sup>+</sup> or both Na<sup>+</sup> and K<sup>+</sup>, the CD spectra dramatically change again, with a disappearance of the maxima at 270 nm and the minima at 235 nm that correspond to the parallel G-quadruplex structure(s), and the emergence of homogeneous antiparallel basket-type characteristics with a distinctive maxima and minima pattern of 292 (+), 262 (−), 245 (+), and 232 (−) nm (shown in dashed red and blue lines, respectively, in Figure 3). The CD spectrum with telomestatin in the presence of both salts (dashed blue line) had a slightly lower maximum at 292 nm than in the presence of telomestatin alone (dashed black line) or K<sup>+</sup> only with telomestatin (dashed red line). Overall, the results from these CD experiments are consistent with telomestatin converting either the randomly structured oligonucleotide or the preformed mixture of G-quadruplexes that are present under K<sup>+</sup> conditions exclusively into the antiparallel basket-type G-quadruplex.

**1.2. Diseleno Sapphyrin (Se2SAP). 1.2.1. Se2SAP in the Presence of K<sup>+</sup> Selectively Converts the Preformed Antiparallel Basket-Type G-Quadruplex to a G-Quadruplex Having Characteristics of a Mixed-Type Hybrid Structure.** The possible induction of a human telomeric intramolecular G-quadruplex structure in the absence of added K<sup>+</sup> or Na<sup>+</sup> but with the addition of the synthetic core-modified porphyrin Se2SAP was monitored using CD spectroscopy (Figure 5A). The CD spectrum of the randomized human telomeric d[T<sub>2</sub>AG<sub>3</sub>]<sub>4</sub> oligonucleotide has a negative band centered at 238 nm, a major positive band at 257 nm, and a minor negative band at 280 nm (Figure 5A, solid black line). Upon addition of excess Se2SAP (5 mol equiv), the CD spectrum changed very little (dashed black line); however, the maximum at 257 nm decreased slightly, a very small positive band evolved between 270 and 300 nm, and the negative band centered at 238 nm shifted to 235 nm. All these small changes could be indicative of only trace amounts of G-quadruplex formation in the presence of Se2SAP.

Similarly, a small but significant change was observed in the CD spectra when excess Se2SAP was added to the preformed antiparallel basket-type G-quadruplex in the presence of Na<sup>+</sup> (Figure 5A; solid and dashed green lines for no drug and drug added, respectively). In contrast, dramatic and pronounced

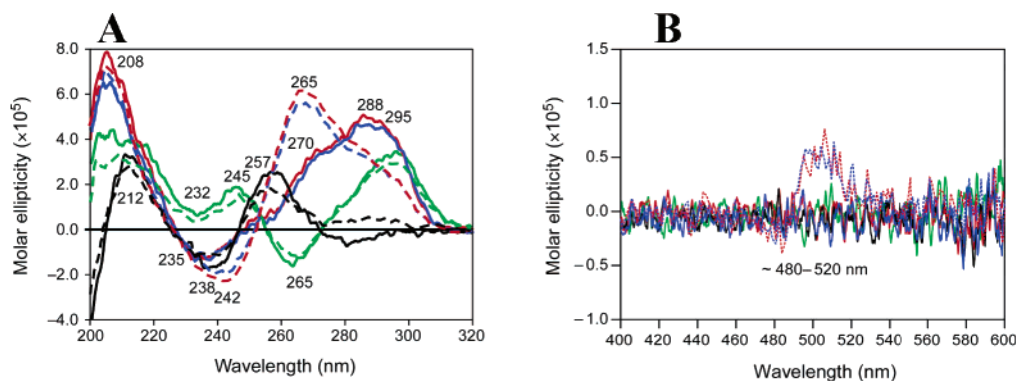


**Figure 5.** (A) CD spectra of  $d[T_2AG_3]_4$  with  $Na^+$  and/or  $K^+$  and Se2SAP. Incubation periods after drug addition were at least 15 min or until no further change in the magnitude of the signal occurred. Line colors: solid black =  $d[T_2AG_3]_4$  (no salt added); dashed black =  $d[T_2AG_3]_4$  + Se2SAP (no salt added); solid red =  $d[T_2AG_3]_4$  + 100 mM KCl; dashed red =  $d[T_2AG_3]_4$  + 100 mM KCl + Se2SAP; solid green =  $d[T_2AG_3]_4$  + 100 mM NaCl; dashed green =  $d[T_2AG_3]_4$  + 100 mM NaCl + Se2SAP; solid blue =  $d[T_2AG_3]_4$  + 100 mM KCl + 100 mM NaCl; dashed blue =  $d[T_2AG_3]_4$  + 100 mM KCl + 100 mM NaCl + Se2SAP. (B) Induced CD signal for  $d[T_2AG_3]_4$  with Se2SAP is observed only in the presence of  $K^+$ . Line colors are the same as for (A).

changes in the CD spectra were observed upon the addition of excess Se2SAP to the preformed mixtures of the G-quadruplexes that were induced in the presence of  $K^+$  only or in the presence of both  $K^+$  and  $Na^+$  (Figure 5A; dashed red and blue lines, respectively). These resulting changes in the CD were typified by the evolution of strong maxima at 265 nm and the significant lowering of the maxima in the 288–295 range. Also, the minima at 238 nm is shifted toward 242 nm. Furthermore, in the presence of  $K^+$ , an induced CD signal for the drug Se2SAP was observed between 480 and 520 nm (Figure 5B, dashed red and blue lines). The induced CD signal is additional evidence for the interaction between the DNA and Se2SAP, since its appearance in the CD spectra is indicative of the change in the chirality of the proximal chemical environment of the Se2SAP.

**1.2.2. Comparison of the CD of the  $d[T_2AG_3]_4$  in  $K^+$  in the Presence of Se2SAP to Other Known G-Quadruplex Structures.** Se2SAP induces a G-quadruplex with both strong parallel (typified by the significant increase in ellipticity of the maximum at 265 nm) and antiparallel (residual ellipticity at a shoulder around 290 nm) characteristics, but only in the presence of  $K^+$  (Figure 5, green line). The persistence of antiparallel characteristics at the end of the titration, in addition to the induced parallel characteristics, is suggestive of a single hybrid structure as the main species or a mixture of two species (i.e., the hybrid- and propeller-type) being formed in solution rather than a simple conversion from the homogeneous antiparallel basket-type to the homogeneous parallel propeller-type G-quadruplex. Significantly, the CD spectrum of this species is similar to the CD spectrum of the  $d[T_2G_4]_4$  oligonucleotide, from the *Tetrahymena* telomeric DNA sequence (Figure 6, red line), although there is a more pronounced shoulder at  $\sim 285$  nm for the Se2SAP-induced structure. The folding pattern of this *Tetrahymena* G-quadruplex is a mixed-type hybrid G-quadruplex with one propeller loop and two lateral loops (Figure 1D). It should be noted that the solution conditions (100 mM NaCl) under which the CD spectrum of this G-quadruplex-forming oligonucleotide was collected were the same as those used by Wang and Patel in their original NMR spectroscopic study of the *Tetrahymena* telomeric DNA.<sup>12</sup> Also included in Figure 6 are the CD spectra of the two other known G-quadruplex solution structures that were solved using NMR spectroscopy, namely the parallel heptad–tetrad G-quadruplex formed in  $K^+$

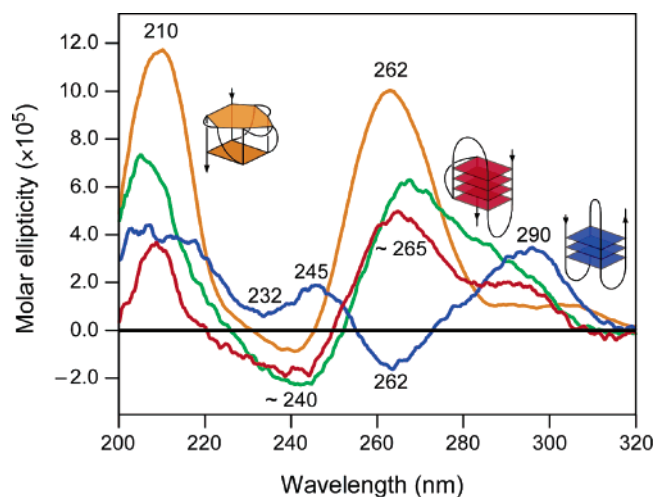


**Figure 6.** Comparison of CD spectra of  $d[T_2AG_3]_4$  in 100 mM NaCl (blue) or in 100 mM KCl with Se2SAP (green),  $d[GGA]_8$  in 100 mM KCl (orange), and  $d[T_2G_4]_4$  in 100 mM NaCl (red).

by the  $d[GGA]_8$  oligonucleotide<sup>22</sup> (orange line) and the antiparallel basket-type G-quadruplex formed in  $Na^+$  by the  $d[T_2AG_3]_4$  oligonucleotide (blue line) (the NMR study in this case was of a 3.5-copy of the human telomeric repeating motifs<sup>15c</sup>). In our comparison of the four oligonucleotides formed by G-quadruplexes, similar concentrations ( $\sim 12.5 \mu M$  in each case) and standard equilibration conditions of 1 day at room temperature were used prior to analysis.

Signature patterns of maxima and minima can be observed for the homogeneous parallel (orange) and antiparallel (blue) G-quadruplexes (Figure 6). Strong maxima at 210 and 262 nm and a shallow minimum at 240 nm are distinctive for the parallel heptad–tetrad G-quadruplex. Similarly, a maximum at approximately 290 nm with a minimum at 262 nm and two small maxima and minima at 245 and 232 nm, respectively, as well as a very broad maximum at 210 nm, form a distinctive CD signature pattern for the antiparallel basket-type G-quadruplex. The maxima–minima pattern for the folded mixed-type hybrid from the *Tetrahymena* telomeric  $d[T_2G_4]_4$  oligonucleotide (red line) is a mixture of the two homogeneous parallel and antiparallel patterns and has parallel characteristics below  $\sim 280$

(22) Matsugami, A.; Ouhashi, K.; Ikeda, T.; Okuzumi, T.; Sotoya, H.; Uesugi, S.; Katahira, M. *Nucleic Acids Res.* **2002**, *2*, 49.



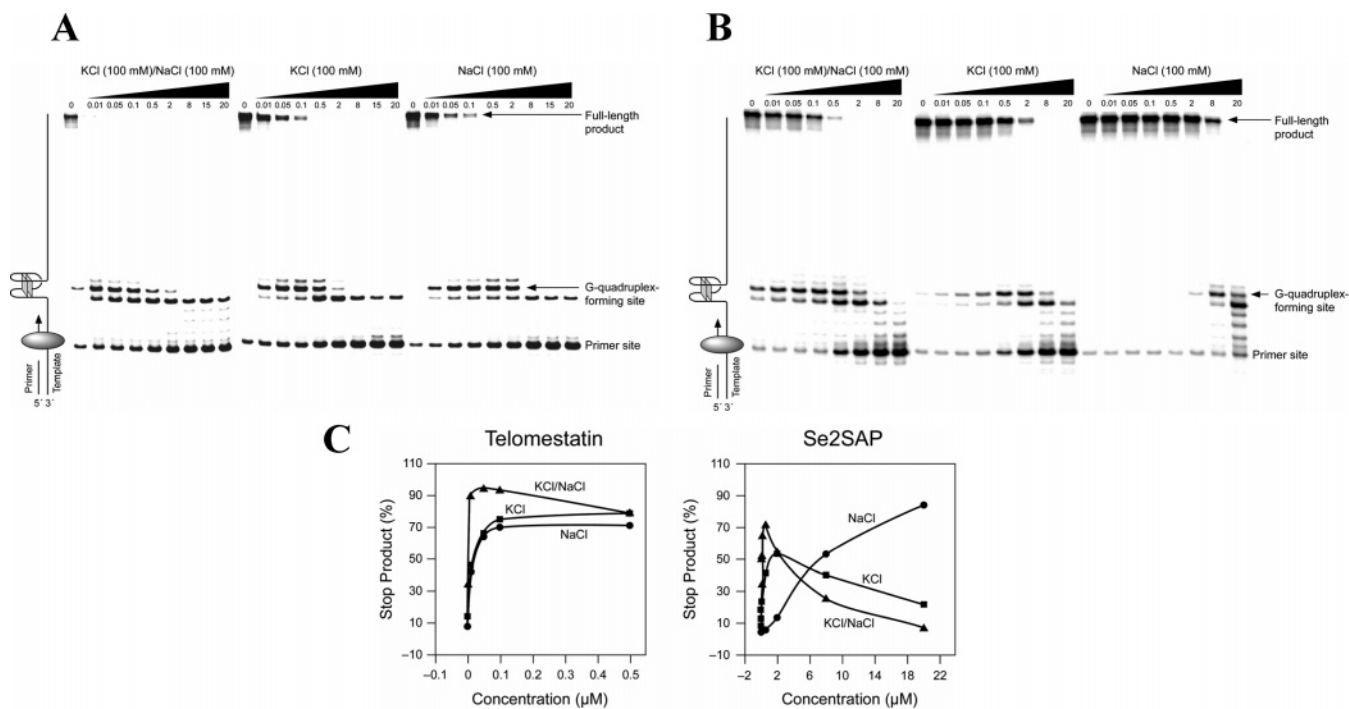


**Figure 7.** Concentration-dependent inhibition of *Taq* polymerase DNA synthesis by stabilization of the human telomeric G-quadruplex structure with (A) telomestatin (0–20  $\mu\text{M}$ ) and (B) Se2SAP (0–20  $\mu\text{M}$ ), using a DNA template containing the human telomeric sequence at 37 °C in 100 mM KCl, 100 mM NaCl, and 100 mM KCl/100 mM NaCl mixture. The illustration to the left of each gel illustrates the principle of the polymerase stop assay. (C) Graphical representations of the quantification of the autoradiograms in (A) and (B), showing the normalized percentage of stop product at the G-quadruplex as a function of concentration ( $\mu\text{M}$ ).

nm, with a distinctly antiparallel maximum between 280 and 300 nm. The CD spectrum of the Se2SAP-induced G-quadruplex under  $\text{K}^+$  conditions (solid red line) best matches the key signature maxima and minima of the folded  $\text{d}[\text{T}_2\text{G}_4]_4$  oligonucleotide CD pattern of all three CD spectra presented in Figure 6. Thus it seems likely that the major species induced by Se2SAP in the presence of  $\text{K}^+$  is the mixed-type hybrid G-quadruplex with one propeller loop and two lateral loops, or, alternatively, is a mixture of species.

**2. Polymerase Stop Assay Studies.** To gain further insight into the selective action of telomestatin and Se2SAP with the human telomeric sequence, a *Taq* polymerase stop assay was used in which the binding in different salt conditions was explored.<sup>23</sup> A primer extension assay was used to measure the drug-induced stability of the telomeric G-quadruplex formed in the template strand (see illustration on left side of gel in Figure 7, A and B). In a typical experiment, polymerase stop product at the G-quadruplex-forming site occurs first at the lower drug concentrations, and then at higher concentrations product accumulates at the primer site, most likely due to drug binding to the primer/template duplex, preventing further polymerase extension. Three different salt conditions were used to mimic the different conditions used in the CD studies. In a mixture of 100 mM KCl and NaCl, in which CD studies show conversion by telomestatin of the mixture of species to the basket structure, this drug stabilizes the G-quadruplex structure at very low concentrations (i.e., at 0.01  $\mu\text{M}$ ; see Figure 7A, left panel). The same is true for the conditions of 100 mM KCl and 100 mM NaCl, although the conversion requires somewhat higher concentrations of telomestatin (Figure 7A, center and right panels, respectively). In contrast, the results with Se2SAP are

quite different (Figure 7B). In 100 mM NaCl, conditions in which the basket structure predominates, Se2SAP only stabilizes the G-quadruplex at very high concentrations ( $\sim 8 \mu\text{M}$ ). In comparison, in 100 mM KCl, or the salt mixture in which the hybrid predominates with a lesser amount of the basket, there is much stronger binding interaction at lower concentrations of drug ( $< 0.05 \mu\text{M}$ ). A graphical comparison of these results with telomestatin and Se2SAP is shown in Figure 7C.

Collectively, these results correspond to those obtained by CD. While telomestatin is able to bind to the basket form, which predominates in 100 mM NaCl, it is able to convert the other form found in 100 mM KCl or the mixed salt to the basket form. In contrast, Se2SAP only binds well to the hybrid form found in 100 mM KCl or in the mixed salt and is unable to convert the basket form found in 100 mM NaCl to the hybrid form.

**3. Surface Plasmon Resonance Studies.** To quantitatively determine the equilibrium constant and stoichiometry of binding of Se2SAP to the 5'-d[AGGG(TTAGGG)<sub>3</sub>]-3' oligonucleotide under different salt conditions, SPR experiments were carried out as described.<sup>17,24</sup> SPR is a powerful technique to monitor molecular reactions in real time<sup>19,24</sup> and has been used previously to study the interaction of compounds with the G-quadruplex

(23) Han, H.; Salazar, M.; Hurley, L. H. *Nucleic Acids Res.* **1999**, *27*, 537.

(24) (a) Wang, L.; Bailly, C.; Kumar, A.; Ding, D.; Bajic, M.; Boykin, D. W.; Wilson, W. D. *Proc. Natl. Acad. Sci. U.S.A.* **2000**, *97*, 12. (b) Wang, L.; Carrasco, C.; Kumar, A.; Stephens, C. E.; Bailly, C.; Boykin, D. W.; Wilson, W. D. *Biochemistry* **2001**, *40*, 2511. (c) Mazur, S.; Tanious, F. A.; Ding, D.; Kumar, A.; Boykin, D. W.; Simpson, I. J.; Neidle, S.; Wilson, W. D. *J. Mol. Biol.* **2000**, *300*, 321. (d) Nguyen, B.; Tardy, C.; Bailly, C.; Colson, P.; Houssier, C.; Kumar, A.; Boykin, D. W.; Wilson, W. D. *Biopolymers* **2002**, *63*, 281. (e) Lacy, E. R.; Le, N. M.; Price, C. A.; Lee, M.; Wilson, W. D. *J. Am. Chem. Soc.* **2002**, *124*, 2153. (f) Carrasco, C.; Faconpré, M.; Chisholm, J. D.; Van Vranken, D. L.; Wilson, W. D.; Bailly, C. *Nucleic Acids Res.* **2002**, *30*, 1774.



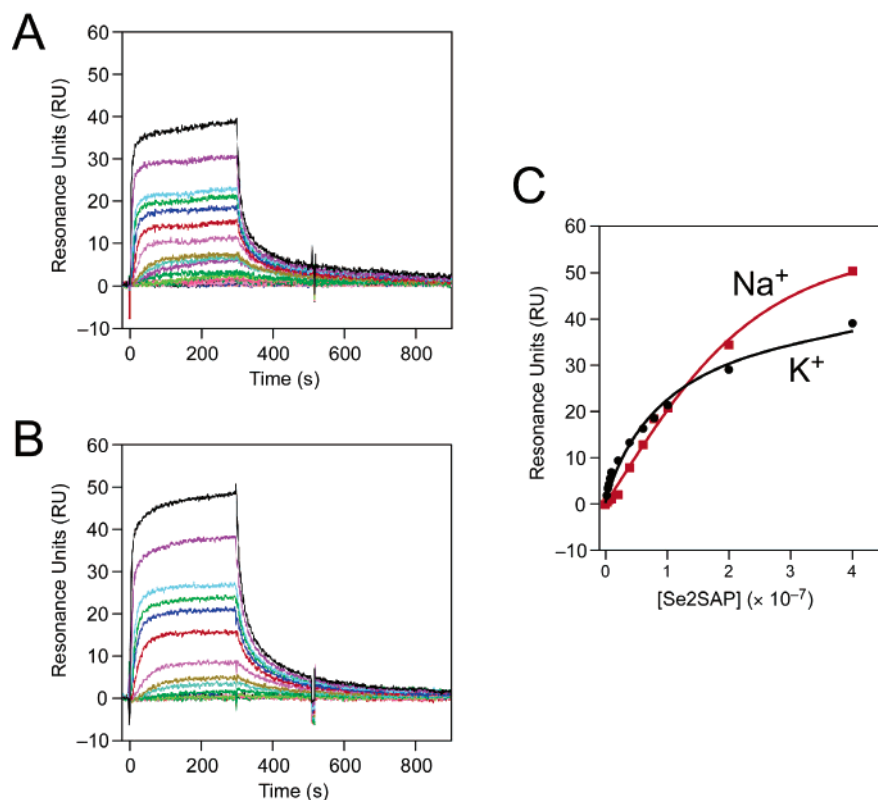


**Figure 8.** SPR sensorgrams for binding of Se2SAP to the immobilized G-quadruplex formed by the human telomeric sequence in the presence of (A) 100 mM of  $K^+$  and (B) 100 mM of  $Na^+$  in HBS at 25 °C. The concentration range is from 0.0  $\mu$ M for the bottom curve to 0.4  $\mu$ M for the top curve in both plots. The glitch at around 500 s is due to required syringe refill. (C) Direct binding plots for Se2SAP binding to the human telomere in  $K^+$  (black  $\bullet$ ) and  $Na^+$  (red  $\blacksquare$ ). The concentration axis is for Se2SAP in the flow solution and is the unbound compound concentration. Direct plot curves from all experiments were fitted to a two-site binding model. The agreement in all experiments was within  $\pm 25\%$  for both  $K$  values.

formed in the human telomeric sequence.<sup>14g,25</sup> This human telomeric oligonucleotide was immobilized in a sensor chip flow cell, and a range of Se2SAP concentrations with  $Na^+$ - or  $K^+$ -containing buffers were injected to quantitatively evaluate the interactions with DNA. The signal in RU was determined as a function of time as the compound flow solution passes over a blank flow cell and the DNA cell. The signal from the blank flow cell was subtracted from that of the DNA cell to provide the final concentration-dependent sensorgrams in Figure 8A,B. As flow continued, a steady-state plateau was reached in which the rates of compound binding to and dissociation from the immobilized DNA were equal. The response values in the steady-state region of the sensorgrams were plotted versus the unbound concentration of Se2SAP from the flow solution ( $C_f$ ) to obtain the binding constants. The stoichiometry of binding arose from the RU value approached with increasing Se2SAP concentration. The significant difference in the limiting RU value for  $K^+$  and  $Na^+$  defined the binding stoichiometry of 2:1 in  $Na^+$  and 1:1 in  $K^+$ .

Binding plots were constructed by averaging the observed SPR response in the steady-state region, and the responses were plotted against  $C_f$  (Figure 8C). The RU versus  $C_f$  plots were fitted to binding models with one or two binding sites (Experimental Procedures). In the case of  $Na^+$  (Figure 8B), the telomeric G-quadruplex sequence binds two molecules of Se2SAP with binding constants that are identical within

experimental error,  $K_1 = K_2 = 4.9 \times 10^6 M^{-1}$ . In contrast, only one strong binding site with  $K_1 = 1.8 \times 10^7 M^{-1}$  for the binding of Se2SAP with the human telomeric sequence in  $K^+$  containing buffer was observed (Figure 8A). The binding isotherms of Se2SAP in  $K^+$  can be fitted to a two-site binding model, but the  $K_2$  is at least 10 times less than the  $K_1$ , characteristic of weak, nonspecific binding, and cannot be determined accurately. The primary equilibrium constant ( $K_1$ ) showed a 4-fold increase in  $K^+$  solution compared to  $Na^+$ , indicating preferential binding of Se2SAP with the hybrid structure rather than with the basket structure. Although the binding constant in  $K^+$  is higher than that in  $Na^+$ , the fitting results do not show a striking visual difference because of the larger second site binding affinity in  $Na^+$ . The SPR results confirm that Se2SAP binds to different G-quadruplex structures formed in the human telomeric sequence in the  $Na^+$  (basket) and the  $K^+$  (hybrid) ions and has a preference for the hybrid structure.

## Discussion

The single-stranded G-rich telomeric 3'-overhang at the ends of chromosomes can form unique secondary DNA structures, such as G-quadruplexes, which are known to inhibit telomerase activity.<sup>6a</sup> Demonstration of the in vivo existence of G-quadruplex structures in telomeres of *Styloynchia macronuclei*,<sup>26</sup> as well as in the promoter regions of oncogenes such as c-MYC<sup>17</sup> in human cells, and the facile interconversion, under physiological conditions, between double- or single-stranded

(25) (a) Teulade-Fichou, M.-P.; Carrasco, C.; Guittat, L.; Bailly, C.; Alberti, P.; Mergny, J.-L.; David, A.; Lehn, J.-M.; Wilson, W. D. *J. Am. Chem. Soc.* **2003**, *125*, 4732.

(26) Schaffitzel, C.; Berger, I.; Postberg, J.; Hanes, J.; Lipps, H. J.; Pluckthun, A. *Proc. Natl. Acad. Sci. U.S.A.* **2001**, *98*, 8572.

DNA and G-quadruplexes, together with their unique structural features, makes G-quadruplexes attractive targets for new anticancer drugs.<sup>6d,e,27</sup> Indeed, a number of small organic molecules that stabilize or induce G-quadruplex structures have been found to inhibit telomerase activity<sup>6</sup> and lower c-MYC levels.<sup>28</sup> In this study, we focused our attention on how different drugs may affect the equilibrium between different G-quadruplex structures derived from human telomeric DNA.

It is clear from our studies that telomestatin and Se2SAP trap out two different G-quadruplex forms from the human telomeric sequence. First, telomestatin most likely traps out the basket form, which has been characterized by NMR spectroscopy, and binds with a 2:1 stoichiometry. However, in the case of Se2SAP, the form trapped out does not appear to correspond to the parallel propeller-type G-quadruplex characterized by X-ray diffraction studies but more likely to a mixed parallel/antiparallel hybrid structure similar to that found in the *Tetrahymena* telomeric DNA sequence. Our observation of two different structures in human telomeric DNA, both having at least some antiparallel characteristics, is not without precedent. Two studies carried out by Balagurumorthy and Brahmachir<sup>20a</sup> and Li et al.<sup>20d</sup> using the 4-copy human telomeric oligonucleotides d[T<sub>2</sub>AG<sub>3</sub>]<sub>4</sub> and d[G<sub>3</sub>(T<sub>2</sub>AG<sub>3</sub>)<sub>3</sub>] (a 3.5-copy variant of the human telomeric sequence), respectively, have reported the same differences between the CD spectra of these oligonucleotides in the presence of Na<sup>+</sup> or K<sup>+</sup>, which are similar to the observations reported here (even with different buffering conditions being taken into account). On the basis of their results obtained from CD analysis as well as other spectroscopic techniques, EMSA, and chemical probing, the supposition was made in both studies that a mixture of different types of G-quadruplex structures was present in the solutions containing K<sup>+</sup>, and the major G-quadruplex was proposed to be an antiparallel intramolecular structure.

What is the identity of the second species trapped out by Se2SAP? We can clearly rule out the parallel propeller structure identified by X-ray studies as the target structure on the basis of the CD studies and energetic conditions, since Se2SAP requires external loops for ionic interactions with the phosphates contained in these loops.<sup>17</sup> CD studies suggest that the form trapped out by Se2SAP is a mixed parallel/antiparallel hybrid

structure similar to the *Tetrahymena* telomeric sequence (Figure 1D). Indeed, Se2SAP binds very well to this species.<sup>17</sup> However, we cannot rule out that there is a mixture of two or more species that gives rise to a composite CD similar to that associated with this hybrid species.

The most important conclusion from this study is that the presence and identity of a ligand can influence the type of G-quadruplex conformations found in solution. It is also likely that crystal packing forces can have equivalent effects on the identity of conformations found. This has significant biological consequences. If a G-quadruplex structure is naturally present in genomic DNA, then its molecular recognition properties will change if the predominant form is changed in the presence of a ligand. This appears to be the case for the c-MYC parallel structure, which is converted into a single or double looped-out structure with Se2SAP and TMPyP4.<sup>17,29</sup> Similarly, intramolecular human telomeric DNA structures will be differentially affected by telomestatin and Se2SAP. As we have previously shown, TMPyP4 is most likely to produce intermolecular structures and associated anaphase bridges, which appear to be absent from cells treated with telomestatin.<sup>16</sup> Thus, while stabilization of G-quadruplex structures is probably a common feature associated with all of these agents, it is only one point of reference when describing the effect of ligands on G-quadruplexes, and it is likely that the biological consequences are a consequence of the structure formed. Studies aimed at determining the G-quadruplex structure(s) naturally present in regions of biological relevance (e.g., telomeres) need to be interpreted with some caution when ligands are present or crystal packing forces may influence the G-quadruplex species found.

**Acknowledgment.** Research was supported by the National Institutes of Health (CA94166). We thank Kazuo Shin-ya (University of Tokyo) for providing the telomestatin for this study. We are grateful to David Bishop for preparing, proof-reading, and editing the final version of the manuscript and figures.

**Supporting Information Available:** Complete list of authors for ref 14d. This material is available free of charge via the Internet at <http://pubs.acs.org>.

JA0505088

(27) Hurley, L. H. *Nat. Rev. Cancer* **2002**, *2*, 188.

(28) Siddiqui-Jain, A.; Grand, C. L.; Bearss, D. J.; Hurley, L. H. *Proc. Natl. Acad. Sci. U.S.A.* **2002**, *99*, 11593.

(29) Seenisamy, J.; Rezler, E. M.; Gokhale, V.; Siddiqui-Jain, A.; Tye, D.; Powell, T. J.; Hurley, L. H. *J. Am. Chem. Soc.* **2004**, *126*, 8702.